

# Amygdala and subregion volumes are associated with photoperiod and seasonal depressive symptoms: A cross-sectional study in the UK Biobank cohort

Naif A. Majrashi<sup>1,2</sup>  | Ali S. Alyami<sup>1</sup> | Nasser A. Shubayr<sup>1,3</sup> |  
 Meshaal M. Alenezi<sup>4</sup> | Gordon D. Waiter<sup>2</sup>

<sup>1</sup>Diagnostic Radiography Technology (DRT) Department, Faculty of Applied Medical Sciences, Jazan University, Jazan, Saudi Arabia

<sup>2</sup>Aberdeen Biomedical Imaging Centre, University of Aberdeen, Aberdeen, UK

<sup>3</sup>Medical Research Center, Jazan University, Jazan, Saudi Arabia

<sup>4</sup>Radiology Department, King Khalid Hospital in Hail, Ministry of Health, Hail, Saudi Arabia

## Correspondence

Gordon Waiter, Aberdeen Biomedical Imaging Centre, University of Aberdeen, Lilian Sutton Building, Foresterhill, Aberdeen AB25 2ZD, UK.  
 Email: g.waiter@abdn.ac.uk

## Funding information

Ministry of Health; Jazan University; Roland Sutton Academic Trust, Grant/Award Number: RSAT-0039/R/16

Edited by: John Foxe

## Abstract

Although seasonal changes in amygdala volume have been demonstrated in animals, seasonal differences in human amygdala subregion volumes have yet to be investigated. Amygdala volume has also been linked to depressed mood. Therefore, we hypothesised that differences in photoperiod would predict differences in amygdala or subregion volumes and that this association would be linked to depressed mood. 10,033 participants ranging in age from 45 to 79 years were scanned by MRI in a single location. Amygdala subregion volumes were obtained using automated processing and segmentation algorithms. A mediation analysis tested whether amygdala volume mediated the relationship between photoperiod and mood. Photoperiod was positively associated with total amygdala volume ( $p < .001$ ). Multivariate (GLM) analyses revealed significant effects of photoperiod across all amygdala subregion volumes for both hemispheres ( $p < .001$ ). Post hoc univariate regression analyses revealed significant associations of photoperiod with each amygdala subregion volume ( $p < .001$ ). PLS showed the highest loadings of amygdala subregions in lateral nucleus, ABN, basal nucleus, CAT, PLN, AAA, central nucleus, cortical nucleus and medial nucleus for left hemisphere and ABN, lateral nucleus, CAT, PLN, cortical nucleus, AAA, central nucleus and medial nucleus for right hemisphere. There were no significant associations between photoperiod and mood nor between mood scores and amygdala volumes, and due to the lack of these associations, the mediation hypothesis was not supported. This study is the first to demonstrate an association between photoperiod and amygdala volume. These findings add to the evidence supporting the role of photoperiod on brain structural plasticity.

## KEYWORDS

amygdala subregion, mood, MRI, photoperiod, seasonality, volume

This is an open access article under the terms of the Creative Commons Attribution-NonCommercial-NoDerivs License, which permits use and distribution in any medium, provided the original work is properly cited, the use is non-commercial and no modifications or adaptations are made.

© 2022 The Authors. *European Journal of Neuroscience* published by Federation of European Neuroscience Societies and John Wiley & Sons Ltd.

## 1 | INTRODUCTION

There is evidence showing the impact of changes in environmental factors such as photoperiod on brain morphology. Recent previous studies (Majrashi, Ahearn, & Waiter, 2020; Majrashi, Ahearn, Williams, & Waiter, 2020; Miller et al., 2015) have found that photoperiod (day length) is positively associated with the volume of brain regions such as the hippocampus and brainstem substructures and that individuals exposed to longer photoperiod days exhibited larger hippocampal and brainstem substructure volumes compared with those exposed to shorter photoperiod days. The amygdala, a region responsible for emotion, cognition and social behaviours (Pessoa, 2010), has also been shown to be affected by seasonal differences in photoperiod in animals (Romeo & Sisk, 2001). In particular, hamsters exposed to shorter photoperiod days exhibited smaller volumes compared with those exposed to longer photoperiod days (Cooke et al., 2001, 2002; Romeo & Sisk, 2001). Furthermore, the growth of the ventral medial amygdala has been shown to be affected by changes in photoperiod and that shorter photoperiods delayed the growth by 10%, whereas longer photoperiods recovered the growth by 22%–25% (Cooke et al., 2007). It has been suggested that these changes in brain volume may be due to the reduction in dendritic spine density in brain substructures. For example, the change in hippocampal volume has been suggested to be due to the reduction in dendritic spine density in the CA-1 and CA-3 substructures measured during short photoperiods (Pyter et al., 2005; Workman et al., 2011), suggesting that seasonal variations in dendritic complexity in amygdala subregions may result in global amygdala volume differences. Overall, these previous mammal studies point to consistent seasonal differences in amygdala volume that have yet to be explored in humans.

Seasonal variations in the amygdala may contribute to seasonally occurring phenotypes, including mood. Morphological changes in the amygdala have been implicated in seasonal depressive-like and anxiety-like behaviours. Mice exposed to shorter photoperiod days exhibited increased aggressive behaviour, fear memory and dendritic spine density of the neurons of the basolateral amygdala compared with those exposed to longer photoperiod days (Silva et al., 2010; Walton et al., 2012). Further, a previous mammal study (Wen et al., 2004) found that hamsters exposed to shorter photoperiods exhibited less neuronal nitric oxide synthase (nNOS), an enzyme implicated in aggressive behaviour, neuronal NOS-immunoreactive cells in the anterior and basolateral amygdaloid areas and were more aggressive compared with those exposed to longer photoperiods. These

previous mammal studies suggest that seasonal changes in amygdala volume are linked to depressive like behaviours. Based on this suggestion, it is plausible that seasonal differences in amygdala volume may contribute to the high prevalence of seasonal variation in mood among humans. A previous study (Kasper et al., 1989) found that up to 92% of community residents report some degree of lower mood during shorter photoperiod days and an increase in mood during longer photoperiod days. Importantly, the majority of the literature demonstrates that changes in the amygdala and subregion volumes are linked with depression (Burke et al., 2011; Sheline et al., 1998) and that depressed subjects exhibited decreased whole amygdala subregion volumes compared with healthy subjects. Therefore, seasonal differences in mood may be partly due to seasonal differences in amygdala volume.

In humans, seasonal morphological differences in brain volume, particularly the brainstem, have been implicated in seasonal depressive symptoms. Brainstem volume was found to mediate the relationship between seasonal differences in photoperiod and depressive symptoms, including low mood and anhedonia, in females but not in males (Majrashi, Ahearn, & Waiter, 2020). In light of the importance of the amygdala to mood regulation and the lack of research linking seasonal variations in photoperiod to seasonal variations in mood and amygdala volume, the aims of this study were to (a) test the seasonal pattern of amygdala and subregion volumes; (b) explore whether photoperiod is associated with amygdala and subregion volume, as well as depressive symptoms; and if so, (c) explore whether the effect of photoperiod on mood might be mediated by seasonal variations in amygdala morphology. We predicted that participants scanned on longer photoperiods would have larger amygdala and subregion volumes compared with those scanned on shorter photoperiods and that the seasonality of depressive symptoms is mediated by seasonal differences in amygdala volumes.

## 2 | METHODS

### 2.1 | UK Biobank participants

UK Biobank (UKBB) is a large population-based prospective study, which was established to investigate genetic, environmental and lifestyle determinants of several disabling diseases, with up to 500,000 participants (Allen et al., 2012). The UKBB participants have previously been described in the literature (Allen et al., 2012; Sudlow et al., 2015). In brief, from 2006 to 2010, UKBB recruited 502,524 participants (men and women throughout

England, Wales and Scotland) aged 40–69 years from a total of 9.2 million postal invitations. All participants were living in the United Kingdom and registered with the National Health Service (NHS). The participants attended one of 22 assessment centres across the United Kingdom and completed a range of lifestyle, demographic, health and mood questionnaires, cognitive assessments and physical measures and subsequently brain imaging at a single centre (UK Biobank Coordinating Centre, Adswold, Stockport) between 2014 and 2016 (Sudlow et al., 2015). More details can be found on the UKBB online data showcase (<https://biobank.ndph.ox.ac.uk/ukb/>).

## 2.2 | UKBB imaging sub-cohort

In 2014, UKBB started imaging the participants, aiming to scan 100,000 participants by 2022. The imaging included MRI brain, heart and abdomen, carotid ultrasound and dual-energy X-ray absorptiometry body scans (Miller et al., 2016). The total imaging time was about two and half hours. Participants who were living within 75 miles (120 km) of the imaging centre in Stockport were further invited to take part in the UKBB Imaging study from April 2014 to December 2016. Participants who had metal implants, non-removable metallic items and penetrating metal injury and those who were not able to complete the imaging due to claustrophobia were excluded from the study. In 2016/2017, the imaging data of 10,103 participants aged between 45 and 79 years (mean = 62.4, SD = 7.4) was released and were included in this cross-sectional study. Out of 10,103 participants, 70 participants were excluded from the study because of issues with their T1-weighted MRI structural images. Out of 10,033 participants, 745 participants were excluded because they did not complete their mood measures in the 2 weeks prior to the scanning. All UKBB participants gave written, informed consent. UKBB received ethical approval from the North-West Multi-Centre Research Ethics Committee (11/NW/03820). This research was conducted using the UKBB Resource under Application Number 24089 (PI Waiter).

## 2.3 | Photoperiod calculation

Photoperiod in hours of daylight on the day of scan was derived from the latitude and longitude information of the location of residence for each participant determined by the 'season' package in R (<https://www.r-project.org/>). Photoperiod in hours was calculated by subtracting sunset from sunrise on the day of scan.

## 2.4 | Mood variable

Mood outcomes composed of scores reflecting the frequency of low mood, anhedonia, tenseness and tiredness over 2 weeks before the assessment. Participants were asked to indicate how often they experience these depressive symptoms including low mood, anhedonia, tenseness and tiredness over the previous 2 weeks during a computerised touchscreen assessment. They were asked the following questions: (a) 'Over the past 2 weeks, how often have you felt down, depressed or hopeless?' for low mood, (b) 'Over the past 2 weeks, how often have you had little interest or pleasure in doing things?' for anhedonia, (c) 'Over the past 2 weeks, how often have you felt tense or restless?' for tenseness and (d) 'Over the past 2 weeks, how often have you felt tired or had little energy?' for tiredness. One additional score was a total depressive symptoms score (ranged from 0 to 12), and it was calculated by summing all the scores of the four depressive symptoms. Participants responded with the following: 'not at all', 'several days', 'more than half the days' and 'nearly every day'. These responses were coded from 0 to 3, respectively, (i.e. 0 = *not at all*, 1 = *several days*, 2 = *more than half the days* and 3 = *nearly every day*). These coded responses were derived directly from the Patient Health Questionnaire (PHQ-9), instrument for depression screening (Spitzer et al., 1999, 2000).

## 2.5 | MRI acquisition

MRI scans were acquired using a 3T Siemens Skyra with a standard Siemens 32-channel RF receive head coil (Miller et al., 2016). T1-weighted three-dimensional (3D) magnetisation-prepared rapid gradient echo (MPRAGE) images were acquired in the sagittal plane within 5 min with these parameters: resolution  $1 \times 1 \times 1$  mm, TR = 2000 ms, TI = 880 ms, field of view  $208 \times 256 \times 256$  mm, iPAT = 2, superior inferior field of view 256 mm (Miller et al., 2016).

## 2.6 | Volumetric analysis and segmentation

Volumetric processing and segmentation were performed using a developmental version of FreeSurfer v6.0 (developmental version of v6.0, which is now a part of a new version of FreeSurfer V7.1.1) software package (<http://surfer.nmr.mgh.harvard.edu>), with amygdala segmentation (Saygin et al., 2017). We chose FreeSurfer because it has longitudinal reproducibility in cortical and subcortical segmentations (Glatard et al., 2015; Khan et al., 2008;

Liem et al., 2015; Ochs et al., 2015; Reuter et al., 2012) and very good reliability in morphometric measurements across scanner manufacturers and field strengths (Han et al., 2006; Reuter et al., 2012). In addition, it has good reproducibility in subcortical segmentations compared with other automated methods (Velasco-Annis et al., 2018). FreeSurfer was used to process the data including averaging volumetric T1-weighted images, motion correction, transformation to Talairach image space, non-uniform intensity normalisation for intensity inhomogeneity correction, removal of non-brain tissues using hybrid watershed and segmentation of subcortical volumetric structures: white matter and deep grey matter (Dale et al., 1999; Fischl et al., 2002; Ségonne et al., 2004).

Total amygdala and subregion volumes were segmented using a novel automated algorithm from FreeSurfer (developmental version of 6.0v) (Saygin et al., 2017). The basis of the segmentation algorithm is based on combining manual labels from ex vivo (10 autopsy samples scanned at ultrahigh-resolution [0.1 mm at 7 T]) and in vivo T1 MRI scans (39 scans) of the whole brain (1-mm resolution) to establish an atlas of the amygdala subregion with a new Bayesian inference algorithm to detect local variations in MRI contrast (Saygin et al., 2017). The FreeSurfer algorithm results in the segmentation of nine distinct amygdala subregions per hemisphere, and these include the lateral nucleus, basal nucleus, accessory basal nucleus, anterior amygdaloid area (AAA), cortical nucleus, medial nucleus, central nucleus, cortical amygdaloid transition area (CAT) and para-laminar nucleus (Figure 1). The accuracy of the segmentation of all amygdala subregion volumes has been validated against the publicly available ADNI and ABIDE neuroimaging datasets, with standard resolution T1 data (Saygin et al., 2017). Therefore, we included all amygdala

subregion volumes in the current analysis. For each subject, volumetric data for the amygdala subregion volumes were calculated using the software's automatic Bayesian segmentation technique. Volumetric data for the amygdala subregion volumes were extracted from FreeSurfer and used for statistical analyses. Brain volumes including total brain volume (TBV) and intracranial volume (ICV) were also calculated by FreeSurfer using the Talairach transformation matrix created from the registration of normalisation and MNI atlas (Buckner et al., 2004). All segmentations for the amygdala were visually checked for errors. No manual interventions were performed on the data. No outliers were detected.

## 2.7 | Statistical analyses

Statistical analyses were conducted using SPSS Version 24, with an alpha for all analyses of  $p = .05$ . The results were thresholded by the standard criterion for correction for multiple comparisons (Bonferroni correction) to minimise the likelihood of Type I (false positive) statistical errors (Armstrong, 2014). In multiple regression analyses investigating the association between photoperiod and total amygdala volume, the threshold of  $p$ -value was  $(.05/3) = <.016$ .

To investigate the association of photoperiod with depressive symptoms including low mood, anhedonia, tenseness, tiredness and total depressive symptoms score, a negative binomial regression model was used. Likelihood ratio tests for these depressive scores showed that overdispersion was greater than 1, that is, their variance was greater than their mean.

To investigate the seasonality, assuming a sinusoidal pattern, of variables of interest including low mood,

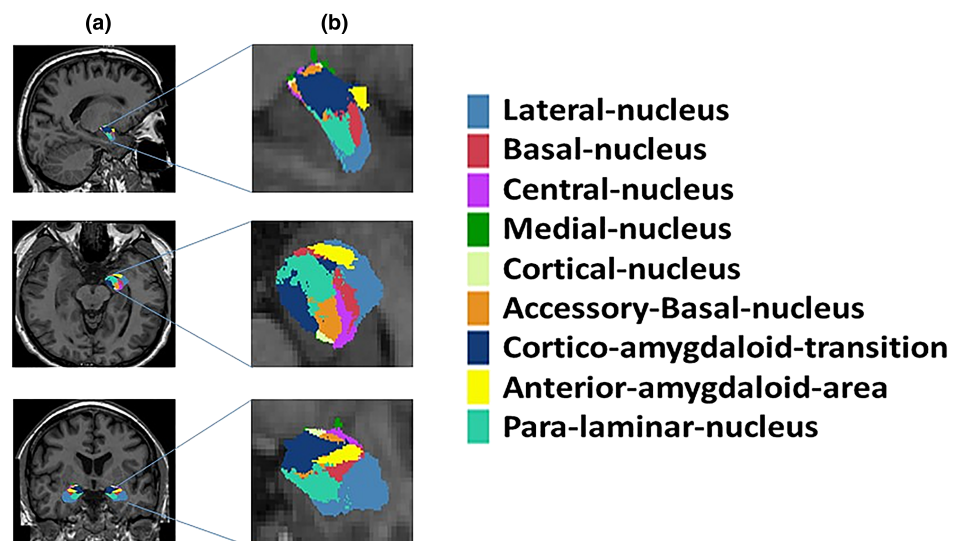


**FIGURE 1** The amygdala subregion segmentations using the developmental version of FreeSurfer; (a) sagittal (top), axial (middle) and coronal (bottom) views displaying the labels of the amygdala subregions and (b) only the subregions marked with different colours

anhedonia, tenseness, tiredness and total depressive score as well as amygdala subregion volumes, a cosinor generalised linear regression (GLM) analysis with sine and cosine functions and month as the time variable (Barnett & Dobson, 2010; Cornelissen, 2014) was used. Sine and cosine transformations of the month of scan were calculated using the formulas

$$\text{Sin} = (2 * \pi(M - 1)/12)$$

$$\text{Cos} = (2 * \pi(M - 1)/12)$$

where M = month of scan (integer number from 1 to 12). We assessed whether the seasonal pattern of the depressive symptoms and amygdala volumes is sinusoidal by comparing a model including sine and cosine month transformations and the covariates of age, ethnicity, Townsend deprivation and living area with models excluding sine and cosine month transformations (Barnett & Dobson, 2010). There were two specific criteria for indicating the significance of seasonality or improved model fit, and these were (a) significance of sine and/or cosine (cosinor) terms ( $p < .05$ ), with amplitude significantly greater than zero and (b) lower Akaike Information Criterion (AIC) for the model including the cosinor terms (Barnett & Dobson, 2010; Lyall et al., 2018). The amplitude of the cosinor model (or curve) was calculated as

$$\sqrt{\beta^2 + \gamma^2}$$

where  $\beta$  and  $\gamma$  are cosine and sine generalised regression coefficients, respectively. Finally, the acrophase ( $\varphi$ ; peak of cosinor model) in month of scan was calculated from

$$\varphi = 12 * \frac{\tan^{-1}(\gamma/\beta)}{2\pi} + 1$$

The seasonal pattern of photoperiod (as a continuous measure of day length) was tested, and it was found that it followed a sinusoidal pattern. No further transforms were applied. Photoperiod was then used as a time variable in all regression analyses instead of the transformed months because photoperiod followed a seasonal pattern.

To examine whether photoperiod was associated with total amygdala volume, first a simple linear regression analysis was performed. Due to previously found associations of age, gender and TBV with amygdala volumes, bivariate correlations with amygdala volumes were performed. Significant correlations were found between age

and TBV and amygdala volumes (see Section 3), and these factors were, therefore, included as covariates to further explore the variance in the amygdala volumes. Then, multiple regression analyses with total amygdala volume as dependent variables, age, gender and TBV as covariates and photoperiod as independent variable were performed.

To account for correlations of photoperiod among the subregion volumes of the amygdala across all participants, a multivariate generalised linear model (GLM) was used. A multivariate GLM included all amygdala subregion volumes as dependent variables, age, gender and TBV as covariates and photoperiod as the independent variable. If the initial multivariate GLM models were significant, then univariate regression model including each amygdala subregion volume as a dependent variable, age, gender and TBV as covariates and photoperiod as the independent variable to assess the correlation between photoperiod and each amygdala subregion volume across all participants was performed.

To examine how the subregion volumes of the amygdala covary with photoperiod when adjusted for age, sex and TBV, a partial least squares (PLS) analysis was used. PLS is a multivariate technique that transforms the predictor (photoperiod) to a smaller set of uncorrelated components and then performs least squares regression on these defined components (Bussy et al., 2021). The main aim of PLS is to identify a set of latent variables (LVs) explaining patterns of covariance between 'subregions' and 'photoperiod' data with the constraint that LVs explain the covariance between the two matrices as much as possible (Chen et al., 2019; Sawatsky et al., 2015). The two input matrices are composed of the 'subregions' and 'photoperiod' data. The 'subregion' data included the volume of each substructure of the amygdala (nine subregions). The 'photoperiod' data contained both photoperiod and covariates (age, sex and TBV) together. A previous study (Chen et al., 2020) has shown that PLS regression can analyse dependent variables when the number of parts of all compositional covariates is higher than the number of observations (the PLS regression between more than one compositional response variable and more than one compositional covariate). Mathematically, each LV will describe linear combinations of the 'substructures' and 'photoperiod' data that maximally covary. A series of PLS analyses were used to investigate (a) the variance accounted for by all left and right amygdala subregion volumes in the first latent factor and (b) the relationships between the amygdala subregion volumes and photoperiod. Each latent factor was then tested statistically by a permutation test (Krishnan et al., 2011; McIntosh & Lobaugh, 2004; McIntosh & Mišić, 2013). Row permutations (5000 iterations) of the

amygdala subregions for both hemispheres and photoperiod were subject to PLS using structural equation modelling (Riou et al., 2016). From these permutation tests, a  $p$ -value was calculated.

For mediation analysis, a standard three-variable path model (Shrout & Bolger, 2002) (photoperiod  $\rightarrow$  amygdala volumes, amygdala volumes  $\rightarrow$  mood and photoperiod  $\rightarrow$  mood) was used to test whether amygdala or subregion volumes mediate the relationship between photoperiod and low mood, anhedonia, tenseness and tiredness. Multiple regression was used to test the association between photoperiod and amygdala volumes (adjusted for age, sex and TBV). Negative binomial regression analysis was used to examine the association between depressive symptoms (adjusted for age, ethnicity, Townsend deprivation index, location of imaging centre and urban-rural settings) and amygdala subregion volumes. Negative binomial regression analysis was used to examine the association between photoperiod and depressive symptoms (adjusted for the above confounders added to TBV). Evidence of mediation is present when the associations between mood and volume and mood and photoperiod are significant. Bootstrapping with 5000 samples was used to compute the 95% confidence interval using the 'PROCESS' method (Preacher & Hayes, 2008) in SPSS Version 24.

### 3 | RESULTS

#### 3.1 | Participant characteristics

A total of 10,033 participants (52.2% females and 47.7% males) ranging in age from 45 to 79 years (mean = 62.5, SD = 7.4) taken from the UKBB cohort were included in the current cross-sectional study. 3D T1-weighted images were collected from all participants. The MRI scans were acquired between May 2014 and December 2016 with the date of scan recorded for each participant. Out of 10,033 participants, only 9289 participants completed a touchscreen questionnaire of their mood in the 2 weeks prior to the MRI assessment. Participants lived in approximately equal proportions north and south of the scanning centre with a mean distance of 31.1 km north or south. Photoperiod for each participant's date of scan was measured based on the location of residence of each participant. The range of observed photoperiod was from 7.25 hours in winter to 17.22 hours in summer. The range for each mood measure was from 0 to 3 (where 0 = *not at all* and 3 = *nearly every day*). Demographic characteristics and amygdala volumes are presented in Table 1.

#### 3.2 | Tests of seasonality of total amygdala and its subregion volumes

A cosinor GLM analysis was used to test whether total or amygdala subregion volumes show a seasonal pattern. We assessed whether significant evidence of seasonality was present by testing whether inclusion of sine and/or cosine transformations of month of scan resulted in improved model fit compared with models not including a month transformation. There were significant cosinor terms for total amygdala (Figure 2) and all subregion volumes (lateral nucleus, basal nucleus, accessory basal nucleus, anterior-amygdaloid-area [AAA] nucleus, central nucleus, medial nucleus, cortical nucleus, cortico-amygdaloidal-transition [CAT] nucleus, para-laminar nucleus) in both hemispheres (Table 2). The peak volume for whole amygdala and most subregion volumes occurred in June. The exceptions were left AAA peak volume that occurred in July and right central nucleus peak volume that occurred in May. The highest amplitude or volume change was found in the lateral nucleus followed by the basal nucleus, accessory basal nucleus and then CAT bilaterally. The right hemisphere showed greater volume difference than the left hemisphere in most regions.

#### 3.3 | Associations of photoperiod with total amygdala and its subregion volumes

##### 3.3.1 | Total amygdala volume associations

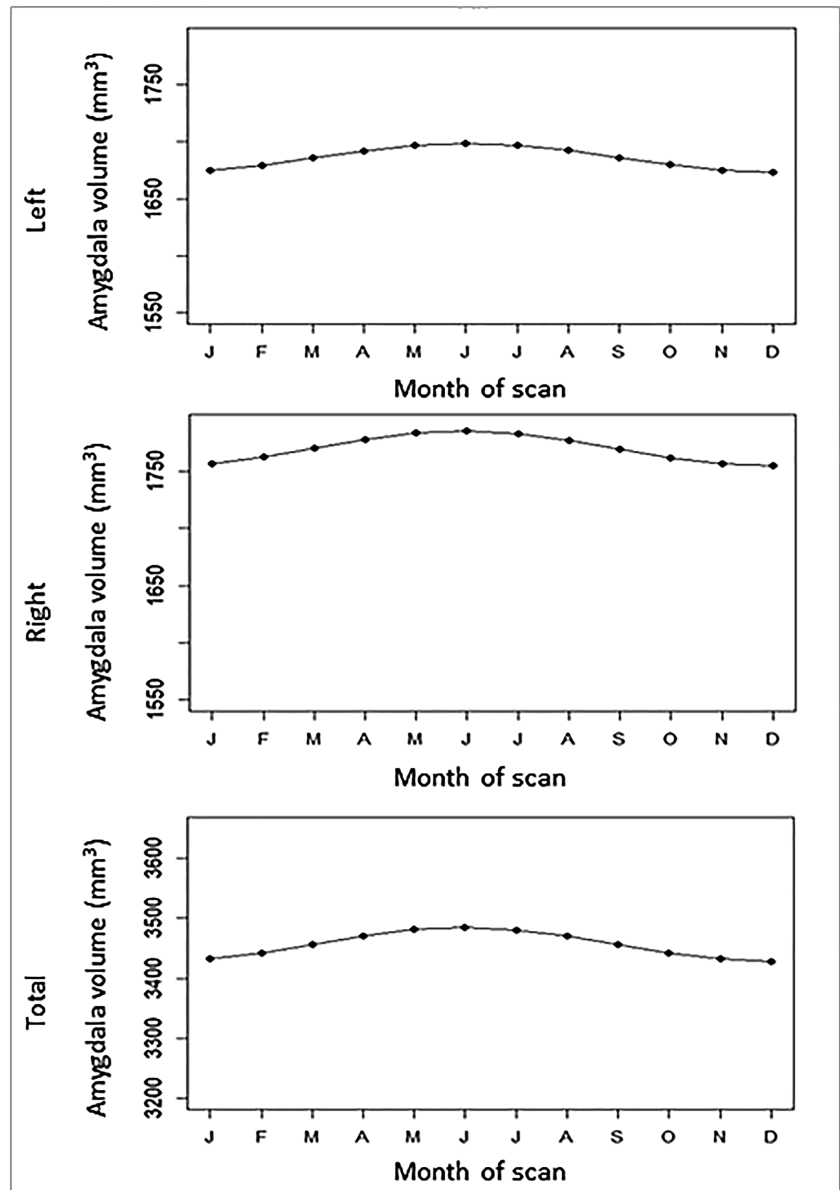
Linear regression revealed significant correlations between photoperiod and total amygdala volume. Photoperiod was positively correlated with left amygdala ( $r(10,033) = .044$ ,  $B = 2.91 \pm .65 \text{ mm}^3/\text{h}$ ), right amygdala ( $r(10,033) = .051$ ,  $B = 3.43 \pm .67 \text{ mm}^3/\text{h}$ ) and total (left + right) amygdala ( $r(10,033) = .050$ ,  $B = 6.34 \pm 1.2 \text{ mm}^3/\text{h}$ ) volumes,  $p < .001$ . To better understand the variance in amygdala volume explained by age, sex and TBV, a multiple regression model was performed. Age, sex and TBV were significantly associated with amygdala volume. When amygdala volume was adjusted for age, sex and TBV in multiple regression models, correlations between photoperiod and left amygdala ( $r(10,033) = .065$ ,  $B = 3.02 \pm .46 \text{ mm}^3/\text{h}$ ), right amygdala ( $r(10,033) = .076$ ,  $B = 3.53 \pm .46 \text{ mm}^3/\text{h}$ ) and total amygdala ( $r(10,033) = .076$ ,  $B = 6.55 \pm .85 \text{ mm}^3/\text{h}$ ) volumes remained significant,  $p < .001$  (Figure 3). When the  $p$ -value was Bonferroni corrected ( $.05/3 = .016$ ), all correlations remained significant,  $p < .016$  (Table 3).

TABLE 1 Characteristics of the UKBB imaging participants with amygdala subregion volumes

Variables	(N = 10,033)	
	Mean	SD
Age (years)	62.53	7.40
Low mood	.211	.500
Anhedonia	.19 1	.450
Tenseness	.240	.520
Tiredness	0.570	.740
Total depressive score	1.212	.760
Townsend deprivation score	-2.010	.560
Photoperiod in hours	13.01	3.05
Rural (number, %)		671 (7.22%)
Urban (number, %)		8553 (92.07%)
Ethnic background: White (number, %)		8728 (93.96%)
Ethnic background: Black (number, %)		29 (0.31%)
Ethnic background: Mixed (number, %)		271 (2.91%)
Ethnic background: Asian (number, %)		191 (2.05%)
Ethnic background: Chinese (number, %)		30 (0.32%)
Ethnic background: Other (number, %)		40 (0.43%)
Left lateral nucleus (mm <sup>3</sup> )	661.20	80.4
Left basal nucleus (mm <sup>3</sup> )	432.14	53.8
Left ABN (mm <sup>3</sup> )	242.28	33.2
Left AAA (mm <sup>3</sup> )	53.16	8.10
Left central nucleus (mm <sup>3</sup> )	42.51	9.10
Left medial nucleus (mm <sup>3</sup> )	18.64	5.71
Left cortical nucleus (mm <sup>3</sup> )	22.00	4.50
Left CAT (mm <sup>3</sup> )	165.52	22.5
Left PLN (mm <sup>3</sup> )	50.88	6.70
Whole amygdala (mm <sup>3</sup> )	1688.37	200.4
Right lateral nucleus (mm <sup>3</sup> )	685.80	81.8
Right basal nucleus (mm <sup>3</sup> )	452.08	54.5
Right ABN (mm <sup>3</sup> )	259.95	34.7
Right AAA (mm <sup>3</sup> )	57.95	8.63
Right central nucleus (mm <sup>3</sup> )	46.84	9.62
Right medial nucleus (mm <sup>3</sup> )	21.49	6.10
Right cortical nucleus (mm <sup>3</sup> )	24.70	4.50
Right CAT (mm <sup>3</sup> )	171.98	22.2
Right PLN (mm <sup>3</sup> )	51.93	6.50
Whole amygdala (mm <sup>3</sup> )	1772.75	205.4
Total (L + R) amygdala	3461.1	390.8
WMV (cm <sup>3</sup> )	470.7	57.2
TGM (cm <sup>3</sup> )	627.1	55.2
TBV (cm <sup>3</sup> )	1097.9	106.9

Abbreviations: AAA, anterior-amygdaloid area; ABN, accessory-basal nucleus; CAT, cortico-amygdaloid transition; GMV, grey matter volume; PLN, paralamellar nucleus; SD, standard deviation; TBV, total brain volume; WMV, white matter volume,

**FIGURE 2** Left, right and total amygdala volumes, fitted with cosinor model to illustrate seasonal pattern



### 3.3.2 | Amygdala subregion volume associations

Multivariate regression analysis revealed significant linear effects of photoperiod across all amygdala subregion volumes (Wilk's lambda = .992;  $F = 9.28$ ;  $df = 9$ ; partial eta squared = .008; observed power = 1.00;  $p < .001$ ) for left hemisphere and (Wilk's lambda = .990;  $F = 10.82$ ;  $df = 9$ ; partial eta squared = .010; observed power = 1.00;  $p < .001$ ) for right hemisphere. Further, individual multiple regression analyses revealed significant linear correlations between photoperiod and amygdala subregion volume in across both hemispheres (Table 3). When the  $p$ -value was Bonferroni corrected ( $.05/54 = .0009$ ), most correlations remained significant

( $p < .0009$ ). The exceptions were the left AAA and right central nuclei.

PLS regression analysis revealed significant latent factors (via a permutation test with 5000 iterations) ( $p = <.001$ ). The first latent factor accounted for 28.6% and 30.8% of variances in the relationship between volume and photoperiod in the left and right amygdala, respectively. PLS showed the strongest associations with photoperiod in the basal nucleus followed by the accessory basal nucleus, lateral nucleus, CAT, PLN, AAA, central nucleus, cortical nucleus and medial nucleus in the left hemisphere and the basal nucleus followed by the accessory basal nucleus, CAT, lateral nucleus, PLN, AAA, cortical nucleus, central nucleus and medial nucleus in the right hemisphere (Figure 4).



TABLE 2 Cosinor parameters and model comparison for (a) left and (b) right amygdala and subregion volumes

Outcome Amygdala subregion	Multivariate generalised regression estimates						$\Delta$ AIC	Acrophase (month)	Amplitude
	Cosine coefficient	(SE)	<i>p</i>	Sine coefficient	(SE)	<i>p</i>			
(a) Left									
Lateral nucleus	−3.74	.841	<.001	2.10	.831	.012	−20.23	June	4.32
Basal nucleus	−3.10	.580	<.001	1.24	.570	.031	−27.2	June	3.31
ABN	−2.34	.360	<.001	1.13	.350	.002	−44.3	June	2.60
AAA	−.221	.102	.031	.042	.100	.233	−.712	July	.236
Central nucleus	−.330	.111	.005	.270	.113	.016	−8.82	June	.434
Medial nucleus	−.392	.071	<.001	.210	.072	.006	−26.0	June	.450
Cortical nucleus	−.353	.056	<.001	.190	.051	.001	−40.9	June	.415
CAT	−1.14	.258	<.001	.670	.257	.008	−20.9	June	1.33
Para-laminar nucleus	−.400	.074	<.001	.130	.075	.079	−24.9	June	.432
Whole amygdala	−12.0	2.06	<.001	6.02	2.03	.003	−36.2	June	13.5
(b) Right									
Lateral nucleus	−5.20	.833	<.001	2.62	.827	.001	−41.8	June	5.80
Basal nucleus	−3.63	.572	<.001	2.06	.565	<.001	−45.4	June	4.12
ABN	−2.06	.369	<.001	1.35	.363	<.001	−38.8	June	2.44
AAA	−.364	.106	.001	.122	.108	.445	−8.3	June	.385
Central nucleus	−.155	.129	.208	.491	.123	<.001	−14.0	May	.527
Medial nucleus	−.280	.084	.001	.225	.083	.007	−14.0	June	.368
Cortical nucleus	−.230	.052	<.001	.211	.050	<.001	−20.3	June	.324
CAT	−1.17	.240	<.001	.486	.240	.048	−20.7	June	1.28
Para-laminar nucleus	−.530	.070	<.001	.236	.070	.001	−53.6	June	.570
Whole amygdala	−13.6	2.04	<.001	7.82	2.01	<.001	−51.8	June	15.7
Total (L + R) amygdala	−25.7	3.80	<.001	13.84	3.73	<.001	−54.9	June	29.1

Notes: Generalised linear regression coefficients (b), robust standard error (SE) and probability of significance (*p*) for cosine and sine transformations of the month of scan. Models were adjusted for age, gender and TBV. AIC values refer to the differences between this model and a model excluding sine and cosine terms but including the covariates (age, sex and TBV). Seasonality of outcome variables (total and left and right amygdala subregion volumes) is inferred from (a) the significance ( $p < 0.05$ ) of the cosine and/or sine generalised linear regression coefficients and (b) improved model fit included cosinor terms by reduced AIC value ( $\Delta$ AIC).

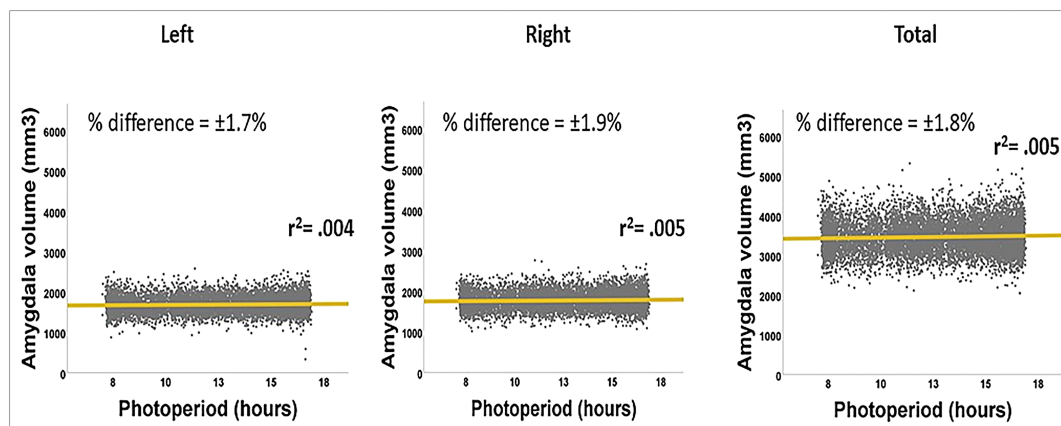


FIGURE 3 Linear correlations between photoperiod and left, right and total amygdala volumes across all participants, + % difference means percentage difference in amygdala volumes from mid-winter (7 h) to mid-summer (17 h), whereas − % difference means percentage difference from mid-summer (17 h) to mid-winter (7 h)

**TABLE 3** Linear correlations between photoperiod and left and right amygdala subregion volumes

Amygdala subregions	(N = 10,033)			
	R	B	SE	p
Left lateral nucleus	.050	.966	.191	<.001
Left basal nucleus	.057	.760	.132	<.001
Left accessory-basal nucleus	.070	.574	.082	<.001
Left AAA	.021	.051	.024	NS
Left central nucleus	.037	.097	.026	<.001
Left medial nucleus	.056	.102	.018	<.001
Left cortical nucleus	.067	.090	.013	<.001
Left CAT	.048	.282	.059	<.001
Left para laminar nucleus	.056	.098	.017	<.001
Left whole amygdala	.065	3.02	.466	<.001
Right lateral nucleus	.069	1.31	.189	<.001
Right basal nucleus	.071	.931	.131	<.001
Right accessory-basal nucleus	.066	.546	.083	<.001
Right AAA	.038	.092	.024	<.001
Right central nucleus	.027	.075	.028	NS
Right medial nucleus	.043	.081	.019	<.001
Right cortical nucleus	.052	.066	.013	<.001
Right CAT	.051	.291	.056	<.001
Right para-laminar nucleus	.077	.130	.017	<.001
Right whole amygdala	.076	3.53	.462	<.001
Total (left + right) amygdala	.076	6.55	.856	<.001

Abbreviations: B, regression coefficient ( $\text{mm}^3/\text{hour}$ ); N, sample number; NS, not significant  $p < .0009$ ;  $p$ , probability of significance; R, Pearson correlation; SE, standard error.

### 3.4 | Association of photoperiod with depressive symptoms

Negative binomial regression was conducted to investigate the association between photoperiod and depressive symptoms including low mood, anhedonia, tenseness, tiredness and total depressive score. There was a significant negative correlation between photoperiod and low mood only ( $p < .05$ ). When corrected for age, sex, ethnicity, living area (urban or rural) and Townsend deprivation index the correlation with low mood did not remain significant (see Table 4).

### 3.5 | Association of amygdala subregion volumes with depressive symptoms

There were no significant correlations between amygdala subregion volumes and depressive symptoms including low mood, anhedonia, tenseness, tiredness and total depressive scores (corrected for age, sex, TBV, ethnicity, urban–rural settings and Townsend deprivation index) across all participants (Table 5).

### 3.6 | Mediation analysis

There was a positive association between photoperiod and amygdala volumes, but there were no significant associations between photoperiod and depressive symptoms nor between amygdala volumes and depressive symptoms. Based on the assumptions of mediation

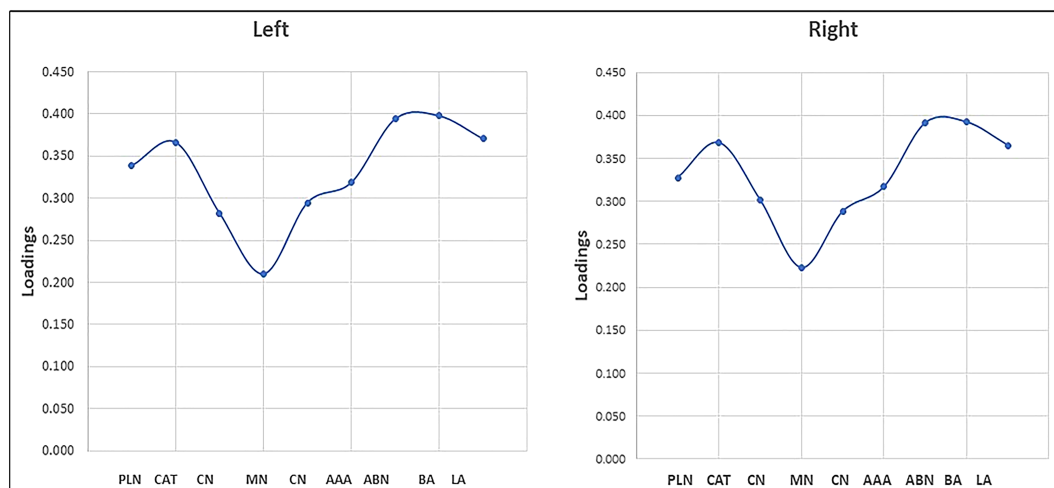


**FIGURE 4** PLS loadings showing most associations with photoperiod across the amygdala subregion volumes in both hemispheres on the first latent variable (LV). Abbreviations: AAA, anterior-amygdaloidal area; ABN, accessory-basal nucleus; BA, accessory nucleus; CAT, cortico-amygdaloidal transition; CeN, central nucleus; Cor, cortical nucleus; LA, lateral nucleus; PLN, para-laminar nucleus

TABLE 4 Associations between photoperiod and all depressive symptoms

	Model		
	b (SE)	IRR	p
Low mood ( <i>n</i> = 9289)	−.015 (0.008)	0.984	.053
Anhedonia ( <i>n</i> = 9289)	−.013 (0.008)	0.987	.122
Tenseness ( <i>n</i> = 9289)	−.007 (0.007)	0.993	.339
Tiredness ( <i>n</i> = 9289)	0.002 (0.005)	1.002	.700
Total depressive score ( <i>n</i> = 9289)	−.005 (0.004)	0.995	.247

Notes: Negative binomial regression coefficients (b), robust standard error (SE) and incidence rate ratios (IRR) for association between photoperiod (corrected for age, sex, ethnicity, living area and Townsend deprivation index) and low mood, anhedonia, tenseness, tiredness and total depressive score.

analysis, there is no evidence that amygdala volume mediates the association between mood and photoperiod.

## 4 | DISCUSSION

To our knowledge, the current study is the first to demonstrate the seasonality of amygdala subregion volumes and test whether the seasonality of depressive symptoms is mediated by seasonal differences in amygdala volumes. We found that amygdala subregion volumes follow a sinusoidal pattern, with the region-dependent peak for amygdala subregion volumes occurring in May, June and July with the highest amplitudes found in the lateral nucleus followed by the basal nucleus, ABN and CAT. This finding extends previous animal findings, which have shown that amygdala volumes in mammals change with season and are larger in the summer months and smaller in the winter months (Cooke et al., 2001, 2002, 2007). This significant association remained when controlling for covariates including age, sex and TBV known to be associated with amygdala volume. The associations between photoperiod and volume were found to be different between the subregions. The basolateral nuclei consisting of the lateral, basal and accessory basal nuclei demonstrated the greatest photoperiodic variations.

The majority of the literature (Cooke et al., 2001, 2002, 2007) have shown that photoperiod is associated with the medial amygdala volume in mammals and that the volume is larger during longer photoperiods and smaller during shorter photoperiods. There is only one previous study (Walton et al., 2012) showing the association of photoperiod with basolateral amygdala neuronal spine density in mammals. This study found that exposure to short photoperiod days increased fear memory in an auditory-cued fear conditioning test and increased dendritic spine density of the neurons of the basolateral amygdala compared with long photoperiod days, suggesting that photoperiodic phenotypic differences in

brain morphology and physiology affect responses to amygdala-related cognitive functions. This evidence, therefore, supports the notion that the functions of amygdala subregions may also be affected by changes in photoperiod. This suggests that the basolateral amygdala functions such as fear memory formation, reward learning and pain regulation may be affected by changes in photoperiod and that these functions are impaired during short photoperiods and improved during long photoperiods.

The associations between photoperiod and total amygdala and subregion volumes were also observed to be different between hemispheres. Right total amygdala and the majority of the subregions displayed greater magnitude of photoperiodic variations, compared with the left amygdala subregions. This finding is consistent with a previous mammal study (Cooke et al., 2002) reporting that seasonal changes in photoperiod affect the volume of the right medial subnucleus of the amygdala, more than the left. A previous study (Wright et al., 2001) found that the right amygdala showed greater habituation to emotional stimuli than the left amygdala, whereas the left amygdala showed more activations to the contrast of fear versus happy emotions, suggesting that the left amygdala is specialised for sustained stimulus evaluation, whereas the right amygdala is part of a dynamic emotional stimulus detection system. In addition, (Baas et al., 2004) found that the left amygdala is more activated in emotional processing regardless of stimulus type, task instructions or habituation rates than the right amygdala. These results suggest that left and right amygdalae play different roles in emotional regulation and that these roles may be differentially affected by seasonal or photoperiodic differences.

Finally, we did not find photoperiod to be associated with mood. This lack of association between mood and amygdala volume contradicts the majority of the literature (Borgsted et al., 2018; Burke et al., 2011; Nolan et al., 2020), which have found amygdala volumes to be smaller in those who are depressed. This lack of

TABLE 5 Associations between amygdala subregion volumes and depressive symptoms

	Low mood		Anhedonia		Tenseness		Tiredness		Total depressive score	
	b (SE)	p	b (SE)	p	b (SE)	p	b (SE)	p	b (SE)	p
Left lateral nucleus	$4.7 \times 10^{-4}$ ( $6 \times 10^{-4}$ )	.435	.001 ( $7 \times 10^{-4}$ )	.383	.001 ( $6 \times 10^{-4}$ )	.321	.001 ( $4 \times 10^{-4}$ )	.123	.001 ( $4 \times 10^{-4}$ )	.107
Left basal nucleus	.001 ( $9 \times 10^{-4}$ )	.287	.001 ( $9 \times 10^{-4}$ )	.458	.001 ( $8 \times 10^{-4}$ )	.481	.001 ( $6 \times 10^{-4}$ )	.085	0.001 ( $5 \times 10^{-4}$ )	.095
Left ABN	.002 (.0014)	.253	.001 (.0015)	.570	.001 (.0013)	.610	$4.6 \times 10^{-4}$ (.0010)	.624	.001 ( $8 \times 10^{-4}$ )	.373
Left AAA	.006 (.0048)	.232	$-7.2 \times 10^{-5}$ (.0053)	.989	.003 (.0047)	.480	.001 (.0034)	.685	.002 (.0028)	.498
Left central nucleus	.004 (.0042)	.359	.003 (.0045)	.445	.002 (.0041)	.555	.003 (.0029)	.333	.003 (.0024)	.252
Left medial nucleus	.008 (.0059)	.166	.003 (.0066)	.693	$-4.8 \times 10^{-4}$ (.0059)	.935	.001 (.0042)	.744	.002 (.0035)	.510
Left cortical nucleus	.008 (.0083)	.349	.006 (.0090)	.522	.002 (.0081)	.768	$-.003$ (.0058)	.550	.001 (.0048)	.868
Left CAT	.001 (.0020)	.604	.001 (.0022)	.629	.001 (.0019)	.653	.002 (.0014)	.199	.001 (.0011)	.235
Left PLN	.005 (.0067)	.498	.007 (.0074)	.311	.003 (.0066)	.692	.012 (.0047)	.054	.008 (.0039)	.063
Left whole amygdala	$2.7 \times 10^{-4}$ ( $2.0 \times 10^{-4}$ )	.268	$2.2 \times 10^{-4}$ ( $3 \times 10^{-4}$ )	.402	$2.0 \times 10^{-4}$ ( $2.0 \times 10^{-4}$ )	.402	$2.6 \times 10^{-4}$ ( $2 \times 10^{-4}$ )	.129	$2.3 \times 10^{-4}$ ( $1 \times 10^{-4}$ )	.102
Right lateral nucleus	$-.001$ ( $6.0 \times 10^{-4}$ )	.056	$-3.1 \times 10^{-4}$ ( $7 \times 10^{-4}$ )	.643	$-4.7 \times 10^{-4}$ ( $6 \times 10^{-4}$ )	.427	$-1.3 \times 10^{-4}$ ( $4 \times 10^{-4}$ )	.751	$-4.2 \times 10^{-4}$ ( $4 \times 10^{-4}$ )	.250
Right basal nucleus	$-.001$ ( $9 \times 10^{-4}$ )	.303	$4.1 \times 10^{-4}$ (.0010)	.672	$7.0 \times 10^{-6}$ ( $9 \times 10^{-4}$ )	.994	$1.4 \times 10^{-4}$ ( $6 \times 10^{-4}$ )	.819	$-4.2 \times 10^{-5}$ ( $5 \times 10^{-4}$ )	.933
Right ABN	$-2.6 \times 10^{-4}$ (.0014)	.849	.002 (.0015)	.244	$1.8 \times 10^{-4}$ (.0013)	.889	$2.1 \times 10^{-4}$ (.0010)	.826	$3.1 \times 10^{-4}$ ( $8 \times 10^{-4}$ )	.687
Right AAA	$-.001$ (.0046)	.828	.003 (.0051)	.591	.003 (.0045)	.452	$-.001$ (.0033)	.690	$2.9 \times 10^{-4}$ (.0027)	.915
Right central nucleus	$1.0 \times 10^{-4}$ (.0040)	.979	.006 (.0043)	.134	.001 (.0039)	.824	.005 (.0028)	.082	.003 (.0023)	.161
Right medial nucleus	.001 (.0058)	.816	.009 (.0063)	.147	.001 (.0059)	.894	.006 (.0041)	.129	.004 (.0034)	.201
Right cortical nucleus	.004 (.0089)	.677	.018 (.0097)	.062	$-.001$ (.0087)	.914	.006 (.0063)	.349	.006 (.0051)	.264
Right CAT	$-3.3 \times 10^{-4}$ (.0020)	.868	.002 (.0022)	.423	$-1.9 \times 10^{-4}$ (.0020)	.921	$2.1 \times 10^{-4}$ (.0014)	.879	$2.2 \times 10^{-4}$ (.0012)	.851
Right PLN	$-.004$ (.0071)	.605	.005 (.0078)	.513	$-.002$ (.0069)	.813	.006 (.0049)	.210	.003 (.0041)	.515
Right whole amygdala	$-2.9 \times 10^{-4}$ ( $2 \times 10^{-4}$ )	0.231	$1.3 \times 10^{-4}$ ( $3 \times 10^{-4}$ )	0.617	$-6.2 \times 10^{-5}$ ( $2 \times 10^{-4}$ )	.796	$3.7 \times 10^{-5}$ ( $2 \times 10^{-4}$ )	.830	$-2.9 \times 10^{-5}$ ( $1 \times 10^{-4}$ )	.834
Total (L + R) amygdala	$-5.1 \times 10^{-6}$ ( $1 \times 10^{-4}$ )	0.970	$1.1 \times 10^{-4}$ ( $1 \times 10^{-4}$ )	0.468	$4.1 \times 10^{-5}$ ( $1 \times 10^{-4}$ )	.751	$8.7 \times 10^{-5}$ ( $9.2 \times 10^{-5}$ )	.347	$5.9 \times 10^{-5}$ ( $7.6 \times 10^{-5}$ )	.439

Notes: Negative binomial regression coefficients (b), robust standard error (SE) for association between amygdala subregion volumes (corrected for age, sex, ethnicity, TBV, urban-rural settings and Townsend deprivation index) and low mood, anhedonia, tenseness, tiredness and total depressive score.

Abbreviations: AAA, anterior-amygdaloid area; ABN, accessory-basal nucleus; CAT, cortico-amygdaloid transition; PLN, para-laminar nucleus.

association between amygdala volume and mood may be explained by a floor effect, where the participants in this cohort reported low average depression symptomology compared with the depressed patients in previous studies. The lack of an association between photoperiod and mood may also be due to the sample size. A previous study (Lyall et al., 2018) found significant associations between changes in photoperiod and some seasonal depressive symptoms such as low mood and anhedonia but with a sample size of more than 70,000.

#### 4.1 | Potential biological mechanisms

The underlying biological mechanisms of seasonal photoperiodic differences in amygdala and subregion volumes in humans are unknown. However, previous animal studies may give some insights. One possibility is that seasonal differences in amygdala volumes may be mediated by effects of hormones. Melatonin has been shown to be directly modulated by changes in photoperiod and mediate many photoperiod-induced adaptations (Zawilska et al., 2007). Previous studies (Adi et al., 2010; Drago & Busa', 2000; Wongprayoon & Govitrapong, 2021) have shown that melatonin receptors are present in the amygdala. The role of melatonin has been examined in the neural song circuitry of songbirds (Bentley et al., 1999). In particular, when European starlings castrated to remove the neuromodulating activity of gonadal steroids were exposed to longer photoperiods, they exhibited increased volume of the song-control nucleus high vocal centre (HVC) compared with those exposed to short photoperiods and that administered exogenous melatonin attenuated the long-day-induced volumetric increase in HVC. These results suggest that there is a role for melatonin in brain plasticity within the central nervous system of vertebrates. Other circulating hormones such as testosterone, oestrogen and corticosterone concentrations, which have been found to be decreased in short-day photoperiods in white-footed mice (Feist et al., 1988), may also modulate morphological amygdala photoperiodic-related differences observed in this study. Siberian hamsters, a rodent that synchronises its reproductive behaviour with season, exposed to shorter photoperiods exhibited smaller somata size and neuronal density of the medial amygdala, which coincided with reduced gonadal weights, seminal vesicles and reduced levels of gonadotropin releasing hormones, compared with those exposed to longer photoperiods (Cooke et al., 1999, 2001, 2002; Gomez & Newman, 1991). Photoperiod has also been shown to effect the sensitivity of the neurons of the medial amygdala subnucleus and that this effect is accompanied with changes in gonadotropin-

releasing hormones (Cooke et al., 2002; Tubbiola et al., 1989). Together, these results may suggest an association between photoperiod, brain volume and testosterone and corticosterone, suggesting that short photoperiods affect the circulation of these hormones, which in turn may alter the morphology of these brain regions. Future research investigating the mechanisms underlying this seasonal plasticity may be important for treating seasonal affective disorders.

Another possibility is that the photoperiodic differences in amygdala subregion volumes may be mediated by the effects of social conditions or interactions. It is known that social interaction influences the brain and that a higher brain density of new neuronal cells has been associated with a higher social interaction (DeVries et al., 1996; Zhao et al., 2003). Importantly, seasonal changes in amygdala volumes have been found to vary depending on social interactions. During short photoperiods, adult male hamsters housed with a female were found to maintain their amygdala volume and gonadal weights compared with those housed in a same-sex environment (Cooke et al., 2001). Together, these results suggest a link between volume of the amygdala, social environment and seasonal changes in photoperiod.

#### 4.2 | Limitations

The current study design has some limitations. Our study was cross-sectional in which participants were measured only once rather than at different times over the year; therefore, the amygdala and subregion volumes measured represent inter-individual variances not changes. Making a causal statement about seasonal change of an individual amygdala volume would require a longitudinal study. Depressive symptom scores in the current study were also taken from questions about feelings over the previous 2 weeks and may be subject to recall bias in reporting mood. Further, the statistical approach of the PLS used in this study has disadvantages that could affect the accuracy of the results. The main limitations of the PLS regression model include risk of overlooking real correlations as well as sensitivity to the relative scaling of the descriptive variables (Cramer, 1993). The PLS composites are derived automatically by the PLS algorithm. In addition, the PLS regression considers the variability of the dependent variables while other models such as principal component regression (PCR) do not. Finally, we included all data available in the January 2017 brain imaging data release. This means that we included participants who may have medical or psychiatric issues related to their brain such as stroke, Alzheimer's disease and congenital or acquired structural brain defects.

## 5 | CONCLUSION

To conclude, the current study is the first to demonstrate that in humans, amygdala and subregion volumes follow a seasonal pattern with a peak in the summer, supporting the animal literature demonstrating that mammals exposed to short photoperiod conditions exhibit smaller amygdala volumes relative to those exposed to long photoperiod conditions. This finding adds to the evidence supporting the role of photoperiod on brain structural plasticity that may have implications for future investigations of changes in mood associated with human exposure to variations in environment, such as natural and artificial light.

### ACKNOWLEDGEMENTS

This research has been conducted using the UK Biobank Resource. This work was supported by the Aberdeen Biomedical Imaging Centre with financial support from the Roland Sutton Academic Trust (RSAT-0039/R/16) and Jazan University and Ministry of Health in Saudi Arabia.

### CONFLICT OF INTEREST

The authors declare that the research was conducted in the absence of any financial or commercial relationships that could be construed as a potential conflict of interest.

### AUTHOR CONTRIBUTIONS

Naif Majrashi carried out the experiments, analysed and interpreted the data and wrote the manuscript. Ali Alyami helped in analysing and interpreting the data. Nasser Shubayr helped in interpreting the data and writing the revised manuscript. Meshaal Alenezi helped in designing the graphs and writing the revised manuscript. Gordon Waiter co-designed the study, co-supervised the project and assisted with experimental interpretation and manuscript preparation.

### PEER REVIEW

The peer review history for this article is available at <https://publons.com/publon/10.1111/ejn.15624>.

### DATA AVAILABILITY STATEMENT

The datasets processed and analysed during the current study are available from the online open access UK Biobank repository (<https://www.ukbiobank.ac.uk/>). This research was conducted under the UK Biobank Resource under Application Number 24089 (PI Waiter).

### ORCID

Naif A. Majrashi  <https://orcid.org/0000-0002-5630-5765>

## REFERENCES

- Adi, N., Mash, D. C., Ali, Y., Singer, C., Shehadeh, L., & Papapetropoulos, S. (2010). Melatonin MT1 and MT2 receptor expression in Parkinson's disease. *Medical Science Monitor: International Medical Journal of Experimental and Clinical Research*, 16(2), BR61–BR67.
- Allen, N., Sudlow, C., Downey, P., Peakman, T., Danesh, J., Elliott, P., Gallacher, J., Green, J., Matthews, P., Pell, J., Sprosen, T., & Collins, R. (2012). UK biobank: Current status and what it means for epidemiology. *Health Policy and Technology*, 1(3), 123–126. <https://doi.org/10.1016/j.hlpt.2012.07.003>
- Armstrong, R. A. (2014). When to use the Bonferroni correction. *Ophthalmic & Physiological Optics: The Journal of the British College of Ophthalmic Opticians (Optometrists)*, 34(5), 502–508. <https://doi.org/10.1111/opo.12131>
- Baas, D., Aleman, A., & Kahn, R. S. (2004). Lateralization of amygdala activation: A systematic review of functional neuroimaging studies. *Brain Research. Brain Research Reviews*, 45(2), 96–103. <https://doi.org/10.1016/j.brainresrev.2004.02.004>
- Barnett, A. G., & Dobson, A. J. (2010). *Analysing seasonal health data*. Springer Berlin Heidelberg.
- Bentley, G. E., Van't Hof, T. J., & Ball, G. F. (1999). Seasonal neuroplasticity in the songbird telencephalon: A role for melatonin. *Proceedings of the National Academy of Sciences of the United States of America*, 96(8), 4674–4679. <https://doi.org/10.1073/pnas.96.8.4674>
- Borgsted, C., Ozenne, B., Mc Mahon, B., Madsen, M. K., Hjordt, L. V., Hageman, I., Baaré, W. F. C., Knudsen, G. M., & Fisher, P. M. (2018). Amygdala response to emotional faces in seasonal affective disorder. *Journal of Affective Disorders*, 229, 288–295. <https://doi.org/10.1016/j.jad.2017.12.097>
- Buckner, R. L., Head, D., Parker, J., Fotenos, A. F., Marcus, D., Morris, J. C., & Snyder, A. Z. (2004). A unified approach for morphometric and functional data analysis in young, old, and demented adults using automated atlas-based head size normalization: Reliability and validation against manual measurement of total intracranial volume. *NeuroImage*, 23(2), 724–738. <https://doi.org/10.1016/j.neuroimage.2004.06.018>
- Burke, J., McQuoid, D. R., Payne, M. E., Steffens, D. C., Krishnan, R. R., & Taylor, W. D. (2011). Amygdala volume in late-life depression: Relationship with age of onset. *The American Journal of Geriatric Psychiatry: Official Journal of the American Association for Geriatric Psychiatry*, 19(9), 771–776. <https://doi.org/10.1097/JGP.0b013e318211069a>
- Bussy, A., Patel, R., Plitman, E., Tullo, S., Salaciak, A., Bedford, S. A., Farzin, S., Béland, M.-L., Valiquette, V., Kazazian, C., Tardif, C. L., Devenyi, G. A., Chakravarty, M. M. (2021). Hippocampal shape across the healthy lifespan and its relationship with cognition. *Neurobiology of Aging*, 106, 153–168. <https://doi.org/10.1016/j.neurobiolaging.2021.03.018>
- Chen, C., Cao, X., & Tian, L. (2019). Partial least squares regression performs well in MRI-based individualized estimations. *Frontiers in Neuroscience*, 13, 1–17. <https://doi.org/10.3389/fnins.2019.01282>
- Chen, J., Zhang, X., & Hron, K. (2020). Partial least squares regression with compositional response variables and covariates. *Journal of Applied Statistics*, 48(16), 3130–3149. <https://doi.org/10.1080/02664763.2020.1795813>

- Cooke, B. M., Hegstrom, C. D., & Breedlove, S. M. (2002). Photoperiod-dependent response to androgen in the medial amygdala of the Siberian hamster, *Phodopus sungorus*. *Journal of Biological Rhythms*, *17*(2), 147–154. <https://doi.org/10.1177/074873002129002438>
- Cooke, B. M., Hegstrom, C. D., Keen, A., & Breedlove, S. M. (2001). Photoperiod and social cues influence the medial amygdala but not the bed nucleus of the stria terminalis in the Siberian hamster. *Neuroscience Letters*, *312*(1), 9–12. [https://doi.org/10.1016/S0304-3940\(01\)02173-5](https://doi.org/10.1016/S0304-3940(01)02173-5)
- Cooke, B. M., Jordan, C. L., & Breedlove, S. M. (2007). Pubertal growth of the medial amygdala delayed by short photoperiods in the Siberian hamster, *Phodopus sungorus*. *Hormones and Behavior*, *52*(3), 283–288. <https://doi.org/10.1016/j.yhbeh.2007.04.008>
- Cooke, B. M., Tabibnia, G., & Breedlove, S. M. (1999). A brain sexual dimorphism controlled by adult circulating androgens. *Proceedings of the National Academy of Sciences of the United States of America*, *96*(13), 7538–7540. <https://doi.org/10.1073/pnas.96.13.7538>
- Cornelissen, G. (2014). Cosinor-based rhythmometry. *Theoretical Biology & Medical Modelling*, *11*, 16. <https://doi.org/10.1186/1742-4682-11-16>
- Cramer, R. D. (1993). Partial least squares (PLS): Its strengths and limitations. *Perspectives in Drug Discovery and Design*, *1*(2), 269–278. <https://doi.org/10.1007/BF02174528>
- Dale, A. M., Fischl, B., & Sereno, M. I. (1999). Cortical surface-based analysis. I. Segmentation and surface reconstruction. *NeuroImage*, *9*(2), 179–194. <https://doi.org/10.1006/nimg.1998.0395>
- DeVries, A. C., DeVries, M. B., Taymans, S. E., & Carter, C. S. (1996). The effects of stress on social preferences are sexually dimorphic in prairie voles. *Proceedings of the National Academy of Sciences of the United States of America*, *93*(21), 11980–11984. <https://doi.org/10.1073/pnas.93.21.11980>
- Drago, F., & Busa, L. (2000). Acute low doses of melatonin restore full sexual activity in impotent male rats. *Brain Research*, *878*(1–2), 98–104. [https://doi.org/10.1016/S0006-8993\(00\)02715-3](https://doi.org/10.1016/S0006-8993(00)02715-3)
- Feist, C. F., Feist, D. D., & Lynch, G. R. (1988). The effects of castration and testosterone on thermogenesis and pelage condition in white-footed mice (*Peromyscus leucopus*) at different photoperiods and temperatures. *Physiological Zoology*, *61*(1), 26–33. <https://doi.org/10.1086/physzool.61.1.30163733>
- Fischl, B., Salat, D. H., Busa, E., Albert, M., Dieterich, M., Haselgrove, C., van der Kouwe, A., Killiany, R., Kennedy, D., Klaveness, S., Montillo, A., Makris, N., Rosen, B., & Dale, A. M. (2002). Whole brain segmentation. *Neuron*, *33*(3), 341–355. [https://doi.org/10.1016/S0896-6273\(02\)00569-X](https://doi.org/10.1016/S0896-6273(02)00569-X)
- Glatard, T., Lewis, L. B., Ferreira da Silva, R., Adalat, R., Beck, N., Lepage, C., Rioux, P., Rousseau, M.-E., Sherif, T., Deelman, E., Khalili-Mahani, N., & Evans, A. C. (2015). Reproducibility of neuroimaging analyses across operating systems. *Frontiers in Neuroinformatics*, *9*. <https://doi.org/10.3389/fninf.2015.00012>
- Gomez, D. M., & Newman, S. W. (1991). Medial nucleus of the amygdala in the adult Syrian hamster: A quantitative Golgi analysis of gonadal hormonal regulation of neuronal morphology. *The Anatomical Record*, *231*(4), 498–509. <https://doi.org/10.1002/ar.1092310412>
- Han, X., Jovicich, J., Salat, D., van der Kouwe, A., Quinn, B., Czanner, S., Busa, E., Pacheco, J., Albert, M., Killiany, R., Maguire, P., Rosas, D., Makris, N., Dale, A., Dickerson, B., & Fischl, B. (2006). Reliability of MRI-derived measurements of human cerebral cortical thickness: The effects of field strength, scanner upgrade and manufacturer. *NeuroImage*, *32*(1), 180–194. <https://doi.org/10.1016/j.neuroimage.2006.02.051>
- Kasper, S., Wehr, T. A., Bartko, J. J., Gaist, P. A., & Rosenthal, N. E. (1989). Epidemiological findings of seasonal changes in mood and behavior. A telephone survey of Montgomery county, Maryland. *Archives of General Psychiatry*, *46*(9), 823–833. <https://doi.org/10.1001/archpsyc.1989.01810090065010>
- Khan, A. R., Wang, L., & Beg, M. F. (2008). FreeSurfer-initiated fully-automated subcortical brain segmentation in MRI using large deformation diffeomorphic metric mapping. *NeuroImage*, *41*(3), 735–746. <https://doi.org/10.1016/j.neuroimage.2008.03.024>
- Krishnan, A., Williams, L. J., McIntosh, A. R., & Abdi, H. (2011). Partial least squares (PLS) methods for neuroimaging: A tutorial and review. *NeuroImage*, *56*(2), 455–475. <https://doi.org/10.1016/j.neuroimage.2010.07.034>
- Liem, F., Méritat, S., Bezzola, L., Hirsiger, S., Philipp, M., Madhyastha, T., & Jäncke, L. (2015). Reliability and statistical power analysis of cortical and subcortical FreeSurfer metrics in a large sample of healthy elderly. *NeuroImage*, *108*, 95–109. <https://doi.org/10.1016/j.neuroimage.2014.12.035>
- Lyall, L. M., Wyse, C. A., Celis-Morales, C. A., Lyall, D. M., Cullen, B., Mackay, D., Ward, J., Graham, N., Strawbridge, R. J., Gill, J. M. R., Ferguson, A., Bailey, M. E. S., Pella, J. P., Curtis, A. M., Smith, D. J., & Smith, D. J. (2018). Seasonality of depressive symptoms in women but not in men: A cross-sectional study in the UK biobank cohort. *Journal of Affective Disorders*, *229*, 296–305. <https://doi.org/10.1016/j.jad.2017.12.106>
- Majrashi, N. A., Ahearn, T., Williams, J. H. G., & Waiter, G. D. (2020). Sex differences in the association of photoperiod with hippocampal subfield volumes in older adults: A cross-sectional study in the UK biobank cohort. *Brain and Behavior*, *10*(6), 01593. Retrieved from <https://abdn.pure.elsevier.com/en/publications/sex-differences-in-the-association-of-photoperiod-with-hippocampa>
- Majrashi, N. A., Ahearn, T. S., & Waiter, G. D. (2020). Brainstem volume mediates seasonal variation in depressive symptoms: A cross sectional study in the UK biobank cohort. *Scientific Reports*, *10*(1), 3592. <https://doi.org/10.1038/s41598-020-60620-3>
- McIntosh, A. R., & Lobaugh, N. J. (2004). Partial least squares analysis of neuroimaging data: Applications and advances. *NeuroImage*, *23*(Suppl 1), S250–S263. <https://doi.org/10.1016/j.neuroimage.2004.07.020>
- McIntosh, A. R., & Mišić, B. (2013). Multivariate statistical analyses for neuroimaging data. *Annual Review of Psychology*, *64*, 499–525. <https://doi.org/10.1146/annurev-psych-113011-143804>
- Miller, K. L., Alfaro-Almagro, F., Bangerter, N. K., Thomas, D. L., Yacoub, E., Xu, J., Bartsch, A. J., Jbabdi, S., Sotiropoulos, S. N., Andersson, J. L. R., Griffanti, L., Douaud, G., Okell, T. W., Weale, P., Dragonu, I., Garratt, S., Hudson, S., Collins, R., Jenkinson, M., ... Smith, S. M. (2016). Multimodal population brain imaging in the UK biobank

- prospective epidemiological study. *Nature Neuroscience*, 19(11), 1523–1536. <https://doi.org/10.1038/nn.4393>
- Miller, M. A., Leckie, R. L., Donofry, S. D., Gianaros, P. J., Erickson, K. I., Manuck, S. B., & Roeklein, K. A. (2015). Photoperiod is associated with hippocampal volume in a large community sample. *Hippocampus*, 25(4), 534–543. <https://doi.org/10.1002/hipo.22390>
- Nolan, M., Roman, E., Nasa, A., Levins, K. J., O'Hanlon, E., O'Keane, V., & Willian Roddy, D. (2020). Hippocampal and amygdalar volume changes in major depressive disorder: A targeted review and focus on stress. *Chronic Stress*, 4, 2470547020944553. <https://doi.org/10.1177/2470547020944553>
- Ochs, A. L., Ross, D. E., Zannoni, M. D., Abildskov, T. J., Bigler, E. D., & For the Alzheimer's Disease Neuroimaging Initiative. (2015). Comparison of automated brain volume measures obtained with NeuroQuant<sup>®</sup> and FreeSurfer: Automated brain volume measures. *Journal of Neuroimaging*, 25(5), 721–727. <https://doi.org/10.1111/jon.12229>
- Pessoa, L. (2010). Emotion and cognition and the amygdala: From “what is it?” to “what's to be done?”. *Neuropsychologia*, 48(12), 3416–3429. <https://doi.org/10.1016/j.neuropsychologia.2010.06.038>
- Preacher, K. J., & Hayes, A. F. (2008). Asymptotic and resampling strategies for assessing and comparing indirect effects in multiple mediator models. *Behavior Research Methods*, 40(3), 879–891. <https://doi.org/10.3758/brm.40.3.879>
- Pyter, L. M., Reader, B. F., & Nelson, R. J. (2005). Short photoperiods impair spatial learning and alter hippocampal dendritic morphology in adult male white-footed mice (*Peromyscus leucopus*). *The Journal of Neuroscience: The Official Journal of the Society for Neuroscience*, 25(18), 4521–4526. <https://doi.org/10.1523/JNEUROSCI.0795-05.2005>
- Reuter, M., Schmansky, N. J., Rosas, H. D., & Fischl, B. (2012). Within-subject template estimation for unbiased longitudinal image analysis. *NeuroImage*, 61(4), 1402–1418. <https://doi.org/10.1016/j.neuroimage.2012.02.084>
- Riou, J., Guyon, H., & Falissard, B. (2016). An introduction to the partial least squares approach to structural equation modelling: A method for exploratory psychiatric research. *International Journal of Methods in Psychiatric Research*, 25(3), 220–231. <https://doi.org/10.1002/mpr.1497>
- Romeo, R. D., & Sisk, C. L. (2001). Pubertal and seasonal plasticity in the amygdala. *Brain Research*, 889(1–2), 71–77. [https://doi.org/10.1016/S0006-8993\(00\)03111-5](https://doi.org/10.1016/S0006-8993(00)03111-5)
- Sawatsky, M. L., Clyde, M., & Meek, F. (2015). Partial least squares regression in the social sciences. *The Quantitative Methods for Psychology*, 11(2), 52–62. <https://doi.org/10.20982/tqmp.11.2.p052>
- Saygin, Z. M., Kliemann, D., Iglesias, J. E., van der Kouwe, A. J. W., Boyd, E., Reuter, M., Stevens, A., Van Leemput, K., McKee, A., Frosch, M. P., Fischl, B., & Augustinack, J. C. (2017). High-resolution magnetic resonance imaging reveals nuclei of the human amygdala: Manual segmentation to automatic atlas. *NeuroImage*, 155, 370–382. <https://doi.org/10.1016/j.neuroimage.2017.04.046>
- Ségonne, F., Dale, A. M., Busa, E., Glessner, M., Salat, D., Hahn, H. K., & Fischl, B. (2004). A hybrid approach to the skull stripping problem in MRI. *NeuroImage*, 22(3), 1060–1075. <https://doi.org/10.1016/j.neuroimage.2004.03.032>
- Sheline, Y. I., Gado, M. H., & Price, J. L. (1998). Amygdala core nuclei volumes are decreased in recurrent major depression. *Neuroreport*, 9(9), 2023–2028. <https://doi.org/10.1097/00001756-199806220-00021>
- Shrout, P. E., & Bolger, N. (2002). Mediation in experimental and nonexperimental studies: New procedures and recommendations. *Psychological Methods*, 7(4), 422–445.
- Silva, A. L., Fry, W. H. D., Sweeney, C., & Trainor, B. C. (2010). Effects of photoperiod and experience on aggressive behavior in female California mice. *Behavioural Brain Research*, 208(2), 528–534. <https://doi.org/10.1016/j.bbr.2009.12.038>
- Spitzer, R. L., Kroenke, K., & Williams, J. B. (1999). Validation and utility of a self-report version of PRIME-MD: The PHQ primary care study. Primary care evaluation of mental disorders. Patient health questionnaire. *JAMA*, 282(18), 1737–1744. <https://doi.org/10.1001/jama.282.18.1737>
- Spitzer, R. L., Williams, J. B., Kroenke, K., Hornyak, R., & McMurray, J. (2000). Validity and utility of the PRIME-MD patient health questionnaire in assessment of 3000 obstetric-gynecologic patients: The PRIME-MD patient health questionnaire obstetrics-gynecology study. *American Journal of Obstetrics and Gynecology*, 183(3), 759–769. <https://doi.org/10.1067/mob.2000.106580>
- Sudlow, C., Gallacher, J., Allen, N., Beral, V., Burton, P., Danesh, J., Downey, P., Elliott, P., Green, J., Landray, M., Liu, B., Matthews, P., Ong, G., Pell, J., Silman, A., Young, A., Sprosen, T., Peakman, T., & Collins, R. (2015). UK biobank: An open access resource for identifying the causes of a wide range of complex diseases of middle and old age. *PLoS Medicine*, 12(3), e1001779. <https://doi.org/10.1371/journal.pmed.1001779>
- Tubbiola, M. L., Nock, B., & Bittman, E. L. (1989). Photoperiodic changes in opiate binding and their functional implications in golden hamsters. *Brain Research*, 503(1), 91–99. [https://doi.org/10.1016/0006-8993\(89\)91708-3](https://doi.org/10.1016/0006-8993(89)91708-3)
- Velasco-Annis, C., Akhondi-Asl, A., Stamm, A., & Warfield, S. K. (2018). Reproducibility of brain MRI segmentation algorithms: Empirical comparison of local MAP PSTAPLE, FreeSurfer, and FSL-FIRST: Comparison of reproducibility of PSTAPLE, FreeSurfer, and FSL-FIRST. *Journal of Neuroimaging*, 28(2), 162–172. <https://doi.org/10.1111/jon.12483>
- Walton, J. C., Haim, A., Spieldenner, J. M., & Nelson, R. J. (2012). Photoperiod alters fear responses and basolateral amygdala neuronal spine density in white-footed mice (*Peromyscus leucopus*). *Behavioural Brain Research*, 233(2), 345–350. <https://doi.org/10.1016/j.bbr.2012.05.033>
- Wen, J. C., Hotchkiss, A. K., Demas, G. E., & Nelson, R. J. (2004). Photoperiod affects neuronal nitric oxide synthase and aggressive behaviour in male Siberian hamsters (*Phodopus sungorus*). *Journal of Neuroendocrinology*, 16(11), 916–921. <https://doi.org/10.1111/j.1365-2826.2004.01248.x>
- Wongprayoon, P., & Govitrapong, P. (2021). Melatonin receptor as a drug target for neuroprotection. *Current Molecular Pharmacology*, 14(2), 150–164. <https://doi.org/10.2174/1874467213666200421160835>
- Workman, J. L., Manny, N., Walton, J. C., & Nelson, R. J. (2011). Short day lengths alter stress and depressive-like responses, and hippocampal morphology in Siberian hamsters. *Hormones and Behavior*, 60(5), 520–528. <https://doi.org/10.1016/j.yhbeh.2011.07.021>



- Wright, C. I., Fischer, H., Whalen, P. J., McInerney, S. C., Shin, L. M., & Rauch, S. L. (2001). Differential prefrontal cortex and amygdala habituation to repeatedly presented emotional stimuli. *Neuroreport*, *12*(2), 379–383. <https://doi.org/10.1097/00001756-200102120-00039>
- Zawilska, J. B., Lorenc, A., Berezińska, M., Vivien-Roels, B., Pévet, P., & Skene, D. J. (2007). Photoperiod-dependent changes in melatonin synthesis in the Turkey pineal gland and retina. *Poultry Science*, *86*(7), 1397–1405. <https://doi.org/10.1093/ps/86.7.1397>
- Zhao, M., Momma, S., Delfani, K., Carlen, M., Cassidy, R. M., Johansson, C. B., Brismar, H., Shupliakov, O., Frisén, J., & Janson, A. M. (2003). Evidence for neurogenesis in the adult mammalian substantia nigra. *Proceedings of the National Academy of Sciences*, *100*(13), 7925–7930. <https://doi.org/10.1073/pnas.1131955100>

**How to cite this article:** Majrashi, N. A., Alyami, A. S., Shubayr, N. A., Alenezi, M. M., & Waiter, G. D. (2022). Amygdala and subregion volumes are associated with photoperiod and seasonal depressive symptoms: A cross-sectional study in the UK Biobank cohort. *European Journal of Neuroscience*, *55*(5), 1388–1404. <https://doi.org/10.1111/ejn.15624>